



**AIAA-93-3092**  
**On Numerical Solutions of Burnett**  
**Equations for Hypersonic Flow Past**  
**2-D Circular Blunt Leading Edges in**  
**Continuum Transition Regime**

X. Zhong  
Univ. of California  
Los Angeles, CA

**AIAA 24th**  
**Fluid Dynamics Conference**  
July 6-9, 1993 / Orlando, FL

# ON NUMERICAL SOLUTIONS OF BURNETT EQUATIONS FOR HYPERSONIC FLOW PAST 2-D CIRCULAR BLUNT LEADING EDGES IN CONTINUUM TRANSITION REGIME

Xiaolin Zhong \*

University of California, Los Angeles, Los Angeles, CA 90024

## Abstract

Using the Burnett equations is one way to advance the continuum approach based on the Navier-Stokes equations into the continuum transition flow regime for rarefied hypersonic flow. Though two-dimensional flow-field numerical solutions of the Burnett equations have been obtained in our previous studies, it is still uncertain how to formulate boundary conditions for the higher-order Burnett equations. Furthermore, few comparative studies have been performed to validate the Burnett equations in multidimensional applications. This paper presents a new method to formulate the additional boundary conditions for the Burnett equations. The new method for the Burnett equations requires the same number of physical surface slip conditions as for the Navier-Stokes equations. We subsequently have obtained numerical solutions of the two-dimensional Burnett equations with the new boundary-condition treatment for hypersonic flow past a cylinder where Knudsen numbers range from 0.02 to 0.4. The results show that the Burnett solutions with the first order slip conditions agree better with DSMC results than the Navier-Stokes solutions do, but the Burnett solutions with the Schamberg second order slip conditions seem to be inaccurate for Knudsen numbers above 0.2.

## I. Introduction

### Motivation

Recently, there have been active research activities in developing theoretical and computational models for nonequilibrium rarefied hypersonic flow because of the development of future hypersonic vehicles, such as the National Aerospace Plane<sup>[1]</sup>. These vehicles are anticipated to involve operations at high atmospheric altitudes where the hypersonic flows around the vehicles belong to the continuum transition regime. The main computational approaches for these nonequilibrium rarefied hypersonic flow are the direct simulation

\* Assistant Professor, Mechanical, Aerospace and Nuclear Engineering Department, Member AIAA

Monte Carlo (DSMC) approach<sup>[2]</sup> and the continuum computational fluid dynamics (continuum CFD) approach. These two approaches are complementary to each other in studying rarefied hypersonic flow at high altitudes.

The DSMC approach, which simulates the gas flow from a molecular point of view, has been the most effective predictive tool for studying rarefied hypersonic flow. Its main disadvantage is the requirement for extremely large computer memory and long computer time. Particularly when the flow approaches the continuum limit, the DSMC approach becomes more and more computationally intensive for practical applications with today's supercomputers. Therefore, the DSMC approach is naturally appropriate for flow with large Knudsen number ( $Kn > 1$ ) and becomes computationally expensive as Knudsen decreases.

On the other hand, the continuum CFD approach, which numerically solves the partial differential equations of macroscopic conservation equations, is much more computationally efficient than the DSMC approach. For flow in the continuum regime with very small Knudsen number ( $Kn < 0.01$ ), the conventional Navier-Stokes equations are the appropriate governing equations. However, as the flow becomes more rarefied and the Knudsen number becomes non negligible, the Navier-Stokes equations become inaccurate. Therefore, the continuum approach is the appropriate approach for flow in the continuum regime and more accurate continuum models than the Navier-Stokes equations are needed as Knudsen increases.

For hypersonic flow in the continuum transition regime, which corresponds to small but non negligible Knudsen numbers, both DSMC and continuum CFD approaches can be used.

This paper is concerned with extending the continuum approach into the transition regime, where the central issue is to develop an advanced set of continuum equations to improve the accuracy of the Navier-Stokes equations near the continuum limit. The goal of our research is to develop a computationally efficient and reasonably accurate computational models for practical multidimensional computations of hypersonic flow fields in this flow regime.

### Research on Burnett Equations

One of the proposed continuum models for hyper-

sonic flow in the continuum transition regime is the Burnett equations<sup>[3]</sup>, which are the continuum conservation equations with higher order stress and heat flux constitutive relations than the Navier-Stokes equations. The Burnett equations were first proposed by Tsien<sup>[4]</sup> in 1946 as constitutive relations for hypersonic slip flow. Subsequent applications of the Burnett equations to hypersonic flow were not successful because of many theoretical and computational difficulties.

There are, among others, two major difficulties in applying the Burnett equations to hypersonic flow,

1. The Burnett numerical solutions for hypersonic flow could not be obtained due to an inherent instability of the equations to high frequency disturbances. This instability precluded any application of the Burnett equations to hypersonic flow computations.
2. There is no generally accepted method for formulating boundary conditions for the Burnett equations. The Burnett equations are a one order higher set of equations than the Navier-Stokes equations. For flow-field computations, the higher order Burnett equations require more boundary conditions in addition to those required for the Navier-Stokes equations. However, there was no clear guide for how to formulate these additional boundary conditions.

The simplest rarefied hypersonic flow problem to test the validity of the Burnett equations is one-dimensional flow structure across shock waves which do not involve the uncertainty of formulating boundary conditions. Early research showed that no hypersonic solutions of the equations could be obtained for even the simple shock structure<sup>[5, 6]</sup> for an upstream Mach number larger than about 1.9. Because of the difficulty in obtaining solutions, the Burnett equations were considered useless<sup>[7, 8]</sup> until the research by Chapman et. al.<sup>[9]</sup> on applying the Burnett equations to one-dimensional shock wave structure in 1988.

In 1988, Fisco and Chapman<sup>[10, 11]</sup> first reinvestigated the Burnett equations and obtained shock-wave solutions of the Burnett equations for some, but not all, monatomic gas models by using a time-marching numerical method. Later, Lumpkin and Chapman<sup>[12]</sup> extended the studies to diatomic gas with a rotational nonequilibrium model and obtained shock-wave solutions of the Burnett equations in nitrogen with coupled translational-rotational nonequilibrium. All their results show that the Burnett equations always agree better with the DSMC results than the Navier-Stokes equations do. These studies, as well as some other studies by Kogan et. al.<sup>[13]</sup>, suggest that the Burnett equations, once considered useless, may be the appropriate governing equations for hypersonic flow in the continuum transition regime.

The studies of Fisco et. al. however, did not solve the two difficulties of the Burnett equations discussed above and therefore their computations had stability difficulties when fine grids were used to compute solutions for the Burnett equations for strong shock waves. This difficulty was analyzed and overcome by Zhong, MacCormack, and Chapman<sup>[14]</sup> in 1991. By using stability analysis of the linearized Burnett equations, they pointed out that the stability difficulties in their computations are caused by the instability of the Burnett equations to disturbances of small wavelengths. This fundamental instability arises in numerical computations when the grid spacing is less than the order of a mean free path, and makes it impossible to use these equations to compute flow with fine resolution and to compute flow in two and three dimensions above a certain altitude for any vehicle. They proposed to stabilize the Burnett equations while maintaining the Burnett level of approximation by augmenting stress and heat flux terms in the Burnett equations with some still higher order terms. Subsequently, they obtained shock wave solutions for all monatomic gas models by using very fine grids, the first known two-dimensional Burnett solutions for hypersonic flow past blunt leading edges, and other two dimensional results<sup>[15]</sup>.

The augmented Burnett solutions for one-dimensional shock structure obtained by Zhong et. al.<sup>[14]</sup> and by Lumpkin et. al.<sup>[16]</sup> agree well with DSMC results. Meanwhile, Pham-Van-Diep et. al.<sup>[17]</sup> also compared the augmented Burnett solutions with their DSMC results for monatomic gases and concluded that the shock shapes are more accurately described by the Burnett equations than the Navier-Stokes equations.

Though the first difficulty of the Burnett equations discussed above has been solved and two-dimensional numerical solutions of the Burnett equations have been obtained, the second difficulty is still a major obstacle in the practical applications of the Burnett equations, i.e., the formulation of boundary conditions for the Burnett equations. In our previous numerical computations of the two-dimensional Burnett equations in [14], the additional boundary conditions on the wall surface are computed by using extrapolation from the interior flow field variables. This boundary condition method is not satisfactory from a theoretical point of view and can raise the question of the uniqueness of the so-obtained solutions.

On the other hand, like the shock wave structure problems, the flow-field solutions of the Burnett equations need to be validated by comparison with either experimental data, or DSMC results. However, only limited comparative studies have been performed to evaluate the merit of these equations in multidimensional applications. The effect of Burnett equations on two-dimensional and three-dimensional hypersonic

transition flow computations has not been fully studied.

## Objectives

This paper is the continuation of our previous studies in applying the Burnett equations to hypersonic flow in the continuum transition regime. The objectives of this paper are to propose a new method in formulating additional boundary conditions for the Burnett equations and to obtain flow-field numerical solutions of the Burnett equations for comparison with DSMC and Navier-Stokes results.

First, we present a new method, which is an extension of the ideas of Schamberg<sup>[18]</sup> and Makashev<sup>[19]</sup> but is much simpler for computations, of specifying additional boundary conditions for the Burnett equations. The new method requires the same number physical slip conditions as those required by the Navier-Stokes equations. The additional boundary conditions for the higher order terms in the Burnett equations are derived from the corresponding Navier-Stokes solutions. The Burnett solutions obtained by using the new boundary condition formulation are accurate up to the Burnett level of approximation to the Boltzmann equation.

Second, we obtain numerical solutions of the two-dimensional Burnett equations with the new formulation of boundary conditions for Mach 11 flow past a cylinder. Computational cases of the flow computed so far have free stream Knudsen numbers ranging from 0.02 to 0.6. For each case, we have computed the solutions of the Navier-Stokes equations, the Burnett equations with the first-order Maxwell/Smoluchowski slip conditions and the Burnett equations with the second-order Schamberg slip conditions. The effect of slip conditions on the solutions are studied. A detailed comparative study on the Burnett, Navier-Stokes, and DSMC solutions are carried out for one of the cases of freestream Knudsen number 0.2. Meanwhile, for other cases, the Burnett solutions are compared with the Navier-Stokes solutions. These results can be used for future comparisons with DSMC results when the later are available.

## II. Governing Equations

### Burnett Equations

It is generally accepted that the governing equation for gas flow ranging from the continuum to the free molecular regime is the Boltzmann equation, which describes the time rate of change of the distribution function due to molecular motion and collisions. The gas flow at both the molecular and macroscopic levels is fully specified by the distribution function, which is the fraction of the particle number in a unit volume in the phase space. The macroscopic flow variables are simply the moments (the averages) of the distribution

function. Multiplying the Boltzmann equation by functions of the molecular velocity  $c_i$  and integrating over the whole velocity space lead to the moment equations of the Boltzmann equation. Specifically, the moment equations of molecular mass, momentum and energy of the Boltzmann equation leads to the macroscopic conservation equations of mass, momentum and energy, i.e., (in two-dimensions):

$$\frac{\partial U}{\partial t} + \frac{\partial F}{\partial x} + \frac{\partial G}{\partial y} = 0 \quad (1)$$

where

$$U = \begin{Bmatrix} \rho \\ \rho u \\ \rho v \\ e \end{Bmatrix} \quad (2)$$

$$F = \begin{Bmatrix} \rho u \\ \rho u^2 + p + \sigma_{11} \\ \rho uv + \sigma_{12} \\ (e + p + \sigma_{11})u + \sigma_{12}v + q_1 \end{Bmatrix} \quad (3)$$

$$G = \begin{Bmatrix} \rho v \\ \rho uv + \sigma_{21} \\ \rho v^2 + p + \sigma_{22} \\ (e + p + \sigma_{22})v + \sigma_{21}u + q_2 \end{Bmatrix} \quad (4)$$

$$p = \rho RT \quad (5)$$

$$e = \rho \left( c_v T + \frac{u^2 + v^2}{2} \right) \quad (6)$$

The conservation equations (1) are the governing conservation equations in the continuum approach and are generally valid for flow from continuum to free molecular regime. However, they do not form a closed set of partial differential equations because the additional stress terms  $\sigma_{ij}$  and heat flux terms  $q_i$  are not given in the conservation equations. Therefore, if Eqs. (1) are solved as the governing equations in the continuum approach, additional equations relating  $\sigma_{ij}$  and  $q_i$  to gradients of macroscopic flow variables, i.e., the constitutive equations, are needed in order to close the equations. It is these constitutive relations that introduce approximation to the generally valid conservation equations.

For gas flow not very far away from equilibrium (small Knudsen numbers), the Boltzmann equation can be solved by the Chapman-Enskog method<sup>[3, 20]</sup>, which is an asymptotic perturbation expansion starting from the equilibrium Maxwellian distribution  $f_0$ ,

$$f = f_0 + f_1 + f_2 + \dots + f_n + O(Kn^{n+1}) \quad (7)$$

where the  $n$  represents the order of approximation with respect to the Knudsen number  $Kn$ . From the distribution function above, we can derive the constitutive

relations for a gas flow at small  $Kn$  as approximate solutions of the Boltzmann equation as follows,

$$\begin{cases} \sigma_{ij} = \sigma_{ij}^{(0)} + \sigma_{ij}^{(1)} + \sigma_{ij}^{(2)} + \sigma_{ij}^{(3)} + \dots \\ q_i = q_i^{(0)} + q_i^{(1)} + q_i^{(2)} + q_i^{(3)} + \dots \end{cases} \quad (8)$$

In Eq. (8), the zeroth order approximation corresponds to the equilibrium flow conditions of the Euler equations, i.e., the stress and heat flux terms vanish. As  $Kn$  increases, the flow departs from thermodynamic equilibrium. Consequently, more and more high order terms in Eq. (8) become significant and are needed to approximate the Boltzmann equation. Retaining the first two terms in Eq. (8) results in the first-order approximation corresponding to the constitutive relations of the Navier-Stokes equations. Similarly, retaining the first three terms in Eq. (8) results in the second-order approximation corresponding to the constitutive relations of the Burnett equations.

The general tensor expressions of the Burnett constitutive relations are as follows,

$$\begin{aligned} \sigma_{ij}^{(B)} = & -2\mu \frac{\overline{\partial u_i}}{\partial x_j} + \frac{\mu^2}{p} \left\{ \omega_1 \frac{\partial u_k}{\partial x_k} \frac{\overline{\partial u_i}}{\partial x_j} \right. \\ & + \omega_2 \left[ -\frac{\partial}{\partial x_i} \left( \frac{1}{\rho} \frac{\partial p}{\partial x_j} \right) - \frac{\partial u_k}{\partial x_i} \frac{\partial u_j}{\partial x_k} - 2 \frac{\overline{\partial u_i} \partial u_k}}{\partial x_k} \right] \\ & + \omega_3 R \frac{\overline{\partial^2 T}}{\partial x_i \partial x_j} + \omega_4 \frac{1}{\rho T} \frac{\partial p}{\partial x_i} \frac{\partial T}{\partial x_j} \\ & \left. + \omega_5 \frac{R}{T} \frac{\partial T}{\partial x_i} \frac{\partial T}{\partial x_j} + \omega_6 \frac{\overline{\partial u_i} \partial u_k}}{\partial x_k} \right\} \end{aligned} \quad (9)$$

and

$$\begin{aligned} q_i^{(B)} = & -\kappa \frac{\partial T}{\partial x_i} + \frac{\mu^2}{\rho} \left\{ \theta_1 \frac{1}{T} \frac{\partial u_k}{\partial x_k} \frac{\partial T}{\partial x_i} \right. \\ & + \theta_2 \frac{1}{T} \left[ \frac{2}{3} \frac{\partial}{\partial x_i} \left( T \frac{\partial u_k}{\partial x_k} \right) + 2 \frac{\partial u_k}{\partial x_i} \frac{\partial T}{\partial x_k} \right] \\ & + \theta_3 \frac{1}{\rho} \frac{\partial p}{\partial x_k} \frac{\overline{\partial u_k}}{\partial x_i} + \theta_4 \frac{\partial}{\partial x_k} \left( \frac{\overline{\partial u_k}}{\partial x_i} \right) \\ & \left. + \theta_5 \frac{1}{T} \frac{\partial T}{\partial x_k} \frac{\overline{\partial u_k}}{\partial x_i} \right\} \end{aligned} \quad (10)$$

where  $\mu$  is the viscosity coefficient,  $\kappa$  is the coefficient of thermal conductivity, and a bar over a derivative designates a nondivergent symmetrical tensor,

$$\overline{A_{ij}} = \begin{cases} \frac{A_{ij} + A_{ji}}{2} - \frac{1}{3}(A_{11} + A_{22} + A_{33}) & \text{if } i = j \\ \frac{A_{ij} + A_{ji}}{2} & \text{if } i \neq j \end{cases}$$

The detailed expressions of the Burnett stress terms written in two-dimensional Cartesian coordinates can be found in [14]. In Eqs. (9) and (10), the coefficients  $\omega_i$ 's and  $\theta_i$ 's can be computed by using the Chapman-Enskog expansion with a molecular repulsive

force model. So far, only the coefficients for the two extreme cases, the hard-sphere and the Maxwellian gas models, have been computed to a high order accuracy as follows:

|            | Maxwell Molecules | Hard-Sphere Molecules |
|------------|-------------------|-----------------------|
| $\omega_1$ | 10/3              | 4.056                 |
| $\omega_2$ | 2                 | 2.028                 |
| $\omega_3$ | 3                 | 2.418                 |
| $\omega_4$ | 0                 | 0.681                 |
| $\omega_5$ | 3                 | 0.219                 |
| $\omega_6$ | 8                 | 7.424                 |
| $\theta_1$ | 75/8              | 11.644                |
| $\theta_2$ | -45/8             | -5.822                |
| $\theta_3$ | -3                | -3.090                |
| $\theta_4$ | 3                 | 2.418                 |
| $\theta_5$ | 117/4             | 25.157                |

The conservation equations (1) together with the Burnett second order constitutive relations given by Eqs. (9) and (10) are termed the Burnett equations. The Burnett stress and heat flux relations consist of the first order Navier-Stokes terms plus second order terms. When the Knudsen number is negligibly small compared to 1, the second order terms are negligible compared with the first order terms and the Burnett equations reduce to the Navier-Stokes equations. However, when the Knudsen number is less than 1 but not negligibly small, the second order stress terms are expected to be non negligible compared to the Navier-Stokes terms, and the Burnett equations are expected to result in second order improvement over the Navier-Stokes equations.

On the other hand, when  $Kn$  is large compared to 1, the flow is in the free molecule regime and the continuum approach herein is not expected to be valid. Therefore, we can only apply the Burnett equations to hypersonic flow in the continuum transition regime.

### Augmented Burnett Terms

It has been shown by Zhong et. al.<sup>[14]</sup> that the linearized conventional Burnett equations are unstable to disturbances of small wavelengths. They subsequently proposed "augmented" Burnett equations to stabilize the conventional Burnett equations while maintaining the second order accuracy of the Burnett level of approximation. The augmented Burnett equations are formed by augmenting the conventional Burnett stress and heat flux terms with some terms of third-order derivatives which are picked from the third order super Burnett equations, but have different coefficients to ensure both analytical and numerical stability. The resulting constitutive relations for the augmented Burnett equations are as follows:

$$\begin{cases} \sigma_{ij} = \sigma_{ij}^{(B)} + \sigma_{ij}^{(a)} \\ q_j = q_j^{(B)} + q_j^{(a)} \end{cases} \quad (12)$$

where the  $\sigma_{ij}^{(B)}$  and  $q_j^{(B)}$  are given by Eqs. (9) and (10), and the augmented terms  $\sigma_{ij}^{(a)}$  and  $q_j^{(a)}$  are

$$\sigma_{ij}^{(a)} = \frac{\mu^3}{p^2} \left\{ \frac{3}{2} \omega_7 RT \frac{\partial}{\partial x_j} \left( \frac{\partial^2 u_i}{\partial x_k \partial x_k} \right) \right\} \quad (13)$$

$$q_i^{(a)} = \frac{\mu^3}{p\rho} \left\{ \theta_7 R \frac{\partial}{\partial x_i} \left( \frac{\partial^2 T}{\partial x_k \partial x_k} \right) + \theta_6 \frac{RT}{\rho} \frac{\partial}{\partial x_i} \left( \frac{\partial^2 \rho}{\partial x_k \partial x_k} \right) \right\} \quad (14)$$

where  $\omega_7 = 2/9$ ,  $\theta_6 = -5/8$ , and  $\theta_7 = 11/16$ .

The Burnett solutions in this paper are the numerical solutions of Eq. (1) together with the constitutive relations given by Eq. (12). We use the augmented Burnett equations to obtain solutions accurate up to the Burnett level of approximation without the instability of the equations to high frequency perturbation.

### III. Boundary Conditions

#### Slip Boundary Conditions

The Chapman-Enskog expansion, which leads to the Navier-Stokes equations and the Burnett equations, results in increasingly higher order sets of partial equations as the order of approximation becomes higher. As a result, the Burnett equations are a one order higher set of equations than the Navier-Stokes equations.

At the Navier-Stokes level of approximation, the equations are second order differential equations, and the boundary conditions on the surface are the velocity slip and temperature jump conditions plus zero normal velocity conditions. The physical slip boundary conditions, which include the velocity slip and temperature jump conditions, can be derived by considering a Knudsen layer flow on the surface<sup>[13]</sup> or by considering momentum and energy balance on the surface<sup>[21]</sup>. Both methods result in similar results for first order slip conditions which are generally termed the *Maxwell/Smoluchowski slip conditions*<sup>[7]</sup>,

$$u_s = \frac{2-\sigma}{\sigma} \lambda \frac{\partial u}{\partial y} + \frac{3}{4} \frac{\mu}{\rho T} \frac{\partial T}{\partial x}, \quad (15)$$

$$T_s = T_w + \frac{2-\alpha}{\alpha} \frac{2\gamma}{(\gamma+1)Pr} \lambda \frac{\partial T}{\partial y} \quad (16)$$

where  $\lambda$  is the mean free path computed by  $\lambda = 16\mu/(5\rho\sqrt{2\pi RT})$ ,  $\sigma$  is the reflection coefficient,  $\alpha$  is the accommodation coefficient, and  $T_w$  is the wall temperature. The slip conditions above have been used extensively in computing slip flow by using the Navier-Stokes equations.

At the Burnett level of approximation, however, the equations are third order differential equations. The only available boundary conditions are the same kind

of slip conditions as those for the Navier-Stokes equations. In principle, the Burnett equations require second order slip conditions derived by solving the Boltzmann equation in the Knudsen layer. However, the only available second order slip conditions were those derived by Schamberg using momentum and energy balance equations with the Burnett molecular distribution on the wall, i.e., the *Schamberg second order slip conditions*<sup>[18]</sup>,

$$u_s = \frac{2-\sigma}{\sigma} \lambda \frac{\partial u}{\partial y} + \frac{3}{4} \frac{\mu}{\rho T} \frac{\partial T}{\partial x} + \left(\frac{\mu}{p}\right)^2 \left[ -\frac{5}{6} RT \left( \frac{\partial^2 u}{\partial y^2} + \frac{\partial^2 v}{\partial x \partial y} \right) + b_1 R \frac{\partial T}{\partial y} \frac{\partial u}{\partial y} - \frac{8}{15} \frac{RT}{\rho} \frac{\partial \rho}{\partial y} \frac{\partial u}{\partial y} - 3a_1 R (RT)^{1/2} \frac{\partial^2 T}{\partial x \partial y} - \frac{3}{2} a_1 R \frac{(RT)^{1/2}}{\mu} \left( \frac{\partial T}{\partial x} \frac{\partial \mu}{\partial y} + \frac{\partial T}{\partial y} \frac{\partial \mu}{\partial x} \right) \right] \quad (17)$$

$$T_s = T_w + \frac{2-\alpha}{\alpha} \frac{2\gamma}{(\gamma+1)Pr} \lambda \frac{\partial T}{\partial y} + \left(\frac{\mu}{p}\right)^2 \left[ e_1 T \left( \frac{\partial u}{\partial y} \right)^2 + e_2 T (RT)^{1/2} \frac{\partial^2 u}{\partial x \partial y} + 2e_3 T (RT)^{1/2} \frac{\partial^2 v}{\partial y^2} + \frac{1}{6\rho} a_1 T (RT)^{1/2} \frac{\partial \rho}{\partial x} \frac{\partial u}{\partial y} - \frac{1}{2\mu} a_1 T (RT)^{1/2} \frac{\partial \mu}{\partial x} \frac{\partial u}{\partial y} + e_4 (RT)^{1/2} \frac{\partial u}{\partial y} \frac{\partial T}{\partial x} + \frac{1}{8\rho} RT \frac{\partial \rho}{\partial x} \frac{\partial T}{\partial x} + e_6 \frac{RT}{\mu} \frac{\partial \mu}{\partial x} \frac{\partial T}{\partial x} + e_6 RT \frac{\partial^2 T}{\partial x^2} + e_7 R \left( \frac{\partial T}{\partial x} \right)^2 + e_8 R \left( \frac{\partial T}{\partial y} \right)^2 - \frac{1}{14} RT \frac{\partial^2 T}{\partial y^2} - \frac{1}{14} \frac{RT}{\mu} \frac{\partial \mu}{\partial y} \frac{\partial T}{\partial y} \right] \quad (18)$$

where,

$$\begin{aligned} a_1 &= \left(\frac{\pi}{2}\right)^{1/2} \left(\frac{2-\sigma}{\sigma}\right) \\ b_1 &= -5.167 \\ e_1 &= -\left[0.31665 + \frac{\pi}{2} \left(\frac{2-\alpha}{\alpha}\right)^2 - \frac{\pi}{4} \left(\frac{2-\alpha}{\alpha}\right) \left(\frac{2-\sigma}{\sigma}\right)\right] \\ e_2 &= -\left(\frac{\pi}{2}\right)^{1/2} \left[\frac{1}{4} \left(\frac{2-\alpha}{\alpha}\right) + \frac{1}{2} \left(\frac{2-\sigma}{\sigma}\right)\right] \\ e_3 &= -\frac{1}{2} \left(\frac{\pi}{2}\right)^{1/2} \left(\frac{2-\alpha}{\alpha}\right) \\ e_4 &= -\left(\frac{\pi}{2}\right)^{1/2} \left[\frac{33}{8} \left(\frac{2-\alpha}{\alpha}\right) - \frac{1}{4} \left(\frac{2-\sigma}{\sigma}\right)\right] \\ e_6 &= 107/56 \\ e_7 &= -7.9888 \\ e_8 &= -5.4912 \end{aligned}$$

The Schamberg slip conditions have only been used in solving slip flows for some simple Couette flows<sup>[18, 22]</sup>. As what will be discussed later, the assumption by Schamberg that the Chapman-Enskog distribution is valid on the wall within the Knudsen layer is questionable. The merit of this assumption can be validated

by comparing Burnett flow-field solutions obtained by using the Schamberg boundary conditions with DSMC results.

For the higher order Burnett equations, it is expected that additional boundary conditions are necessary in order to obtain a unique set of solutions for the Burnett equations. However, there is no physical basis on how to specify the additional boundary conditions. Currently there is no satisfactory method in formulating these additional boundary conditions for the Burnett equations. Two methods to solve the additional boundary conditions problem was proposed by Schamberg<sup>[18]</sup> and by Makashev<sup>[19]</sup> for the Burnett equations.

### Schamberg's Method

Schamberg<sup>[18]</sup> argued that the Burnett equations require the same number of physical surface slip boundary conditions as the Navier-Stokes equations, and the solutions accurate up to the Burnett level of approximation can be obtained by a perturbation series starting with the Navier-Stokes solutions. This expansion solutions of the Burnett equations require no additional boundary conditions for higher order solutions, because at each level of approximation, the higher order derivative terms are evaluated by the known lower level of perturbation solutions.

The assumption of Schamberg's method is that no radical change of the flow pattern is expected when proceeding from the Navier-Stokes solutions to the Burnett solutions in the flow field including the boundary layer. The Burnett solutions are only a small improvement over the Navier-Stokes solutions. This situation is different from the transition from Euler solutions to Navier-Stokes solutions, where a radical change occurs in the appearance of the boundary layer.

Schamberg's method seems to be appropriate, and can be validated by using the DSMC results. However, his method does not solve the simultaneous set of partial differential equations corresponding to the Burnett equations. Instead, the Burnett solutions are solved as perturbation solutions starting from the Navier-Stokes equations. In numerical computations of hypersonic flows, It is more convenient and preferable to solve the Burnett equations as a simultaneous set of equations. If so, Schamberg's method can not be used.

### Makashev's Method

Makashev<sup>[19]</sup> proposed a method to construct additional boundary conditions for the simultaneous Burnett equations. His argument, which is similar to that of Schamberg, that if the Burnett solutions are expanded as a perturbation series using the Navier-Stokes equations as leading terms, no additional boundary conditions are required. But if the Burnett equations are to be solved as a simultaneous set of partial differential equations, additional boundary conditions will

be required. The additional boundary conditions cannot be arbitrarily specified; they must be formulated to be consistent with the expansion solutions so that no singularity caused by the presence of higher derivatives multiplied by small parameters (Knudsen number) will be present. Subsequently, Makashev formulated the additional boundary conditions for second order equations based on the first order solutions. The solutions are accurate up to the second order approximation.

However, the boundary conditions of Makashev involve complicated analyses and his formulas for additional boundary conditions are complicated and are difficult to implement in obtaining numerical solutions for the Burnett equations.

### New Formulation of Boundary Conditions

We propose a new simplified method of formulating the additional boundary conditions for the simultaneous Burnett equations. The new method is an extension of the Schamberg and Makashev's methods but is simpler and easier to implement in numerical computations.

When the Boltzmann equation is solved by using the Chapman-Enskog or the Hilbert method, the perturbation expansion is singular at the wall. The flow field is divided into the outer field, which includes the regular boundary layer, and the inner field, which is a thin layer a few mean free paths thick separating the wall from the outer field. This inner field is termed the Knudsen layer. The Chapman-Enskog expansion, which is an outer expansion based on small Knudsen number, is valid only in the outer field. Therefore, the Chapman-Enskog expansion, as well as the Navier-Stokes and Burnett equations are not valid in the Knudsen layer where the Boltzmann equation has to be used.

In principle, the boundary conditions for the Navier-Stokes equations and the Burnett equations in the outer field can be obtained by the method of matched asymptotic expansion<sup>[23]</sup> between the outer-field Chapman-Enskog distribution and Knudsen layer solutions of the Boltzmann equation. Therefore, it is expected the slip velocity and temperature used as boundary conditions appropriate for the conservation equations in the outer field are different from the actual values on the wall obtained by solving the Boltzmann equation in the Knudsen layer. Figure 1 shows a schematic distribution of velocity across the Knudsen layer and outer field. The boundary condition for the Navier-Stokes equations is the slip velocity,  $u_s$ , which is different from the actual velocity,  $u_0$ , on the wall.

For the flow equations in the outer field, the Chapman-Enskog method leads to increasingly higher order equations which require additional boundary conditions for the higher order terms. However, if the Burnett solutions are expanded as a perturbation series using the Navier-Stokes equations as leading terms, no additional boundary conditions are required.

We use the following ordinary differential equations as an example to demonstrate the idea of formulating additional boundary conditions for outer-field higher order equations,

$$\epsilon y'' + y' = x \quad (19)$$

$$y(0) = 1, \quad y'(0) = 2 \quad (20)$$

where  $\epsilon$  is a small positive number. This equation corresponds to the Boltzmann equation with a singularity on the wall at  $x = 0$ .

Eq. (19) from the inner field to outer field can be solved by a matched asymptotic expansion method. In the outer field, we assume the following outer-field expansion,

$$y_{outer} = y_1 + \epsilon y_2 + \dots \quad (21)$$

Substituting Eq. (21) into Eq. (19) leads to the perturbation equations,

$$y_1' = x \quad (22)$$

$$y_2' = -y_1'' \quad (23)$$

⋮

In the equations above, for  $k$ -th order solution  $y_k$ , the order of differential equations do not increase; the higher order terms only involve the known previous level solutions. Therefore only one boundary condition is needed for every level of approximation of outer-field equations. These boundary conditions can be derived by matching the outer solutions with the inner solutions in the intermediate area between the outer field and inner layer.

In the inner layer on the wall, we introduce a magnified inner coordinates,

$$X = x/\epsilon, \quad Y(X) = y(x) \quad (24)$$

Eq. (19) is transformed in the inner coordinates,

$$Y'' + Y' = \epsilon^2 X \quad (25)$$

$$Y(0) = 1, \quad Y'(0) = 2\epsilon \quad (26)$$

Expanding the inner solutions,

$$Y = Y_1 + \epsilon Y_2 + \dots \quad (27)$$

leads to the perturbation solutions of the inner layer,

$$Y = 1 + \epsilon(2 - 2e^{-X}) + \dots \quad (28)$$

The outer limit of the inner solutions equals to the boundary conditions for the outer solutions at  $x = 0$  as follows,

$$y_{outer}(x=0) = 1 + 2\epsilon + \dots \quad (29)$$

Therefore, the boundary conditions for the outer expansion solutions are  $y_1(0) = 1, y_2(0) = 2, \dots$ . Solving Eqs. (22) and (23) with these boundary conditions leads to the following outer solutions,

$$y_{outer} = (1 + x^2/2) + \epsilon(2 - x) + \dots \quad (30)$$

The outer expansion above is a good approximation except in the inner layer, and it corresponds to the solution obtained by using Schamberg's method of specifying boundary conditions for the Burnett equations.

If the outer equations are to be solved as a simultaneous equation in the outer field corresponding to the Burnett equations, one more boundary condition is needed in addition to the first boundary condition given by Eq. (29). Makashev set the additional boundary condition such that the outer solutions of second order equations do not introduce new singularity on the wall as follows,

$$y'(0) = [x - \epsilon y_1']_{x=0} + 0(\epsilon^2) \quad (31)$$

Makashev's method corresponds to Solving Eq. (19) with boundary conditions given by Eqs. (29) and (31).

However, the additional boundary conditions proposed by Makashev are often not easy to implement for complicated equations such as the Burnett equations. The essential idea of Makashev's boundary conditions is that the second terms on the wall can be evaluated by the known first order solution while maintaining the second order accuracy of the solution. Therefore, we propose the following simple method, which still maintains the second order approximation. The new method evaluated the higher order derivatives on the wall directly by using the first order solutions, i.e.,

$$y'(0) = y_1'(x=0) \quad (32)$$

where  $y_1$  is the first order outer solution given by Eq. (22).

Makashev's method corresponds to Solving Eq. (19) with boundary conditions given by Eqs. (29) and (32). It can be shown that the resulting solutions are accurate up to a second order approximation.

Figure 2 shows the solutions of the ordinary differential equation (19) when  $\epsilon = 0.1$ . The outer expansion solution agrees well with the exact solutions except near the wall in the inner "Knudsen" layer when  $x < 0.25$ . On the other hand, the inner expansion solution agrees well with the exact solutions within the inner layer. The boundary conditions for the outer solutions are provided by matching the inner solutions with the outer solutions. The figure shows that the boundary conditions for the outer expansion equations are different from the actual boundary values on the wall.

The outer solutions obtained by solving the simultaneous outer equations with Makashev's additional boundary conditions (square symbols) and with our new formulation (triangle symbols) are also plotted in the figure. In the figure,  $y_1$  is the first order outer solution. The figure shows that solution obtained by using the new boundary condition formulation agrees very well with the solution obtained by using Makashev method and the exact solution in the outer region.

Following the new formulation above, we can formulate the additional boundary conditions for the Burnett equations. When solving the Burnett equations by using the finite volume method, for example, the flux term  $G$  in Eq. (4) need to be evaluated on the wall at  $y = 0$ . Similar to the analysis of the example above, the new method evaluates the higher order Burnett stress and heat flux terms in  $G$  by using the known values of the corresponding Navier-Stokes solutions. For example,

$$\sigma_{21}^{(B)}|_{y=0} = -2\mu \frac{\overline{\partial u_2}}{\partial x_1} + \frac{\mu_{n-s}^2}{p_{n-s}} \left\{ \omega_1 \frac{\partial u_k}{\partial x_k} \frac{\partial u_i}{\partial x_j} + \dots \right\}_{n-s} \quad (33)$$

where the subscript n-s represents the solutions of the Navier-Stokes solutions, which are the first order solutions.

The other variables in  $G$  are evaluated by using the simultaneous Burnett solutions by using the physical velocity slip and temperature conditions. The method is the similar to that for the Navier-Stokes equations. The difference here is that the Navier-Stokes equations use first order slip conditions appropriate to the Navier-Stokes level of approximation, but the Burnett equations, in principle, should use second order slip conditions appropriate to the Burnett level of approximation.

In principle, the second order slip conditions can be obtained by solving the Boltzmann equation in the Knudsen layer. The second order slip conditions for the Burnett equations outside the Knudsen layer are the results of matching the Knudsen layer solutions and the outer-field Chapman-Enskog distribution in the interaction region between the Knudsen layer and the boundary layer. To our knowledge, however, there has not been any work done in deriving these second order slip conditions based on considering the Boltzmann equation in the Knudsen layer.

In our previous computations of numerical flow-field solutions of the Burnett equations, the additional boundary conditions for the Burnett equations are evaluated by extrapolating the flow variables from the interior of the flow field. Our computations showed that this way of treating the boundary conditions for the Burnett equations are numerically satisfactory. However, this method of extrapolation does not have any analytical foundation and may lead to the problem of non uniqueness of the Burnett equations. Therefore, we replace it by the present formulation based on formal analysis. Comparing the results of the two methods show that Burnett solutions using the extrapolation method agree with those using the new boundary conditions when the Knudsen number is less than about 0.2.

## IV. Numerical Methods

In this paper, the two-dimensional Burnett equations are solved by using a finite volume implicit method<sup>[14]</sup>, which is second order accurate in space and is an extension of the implicit Gauss-Seidel method for the Navier-Stokes equations described by MacCormack<sup>[24]</sup>. The inviscid terms in the conservation equations are computed by using the second order modified flux-splitting method proposed by MacCormack<sup>[24]</sup>, and all the viscous terms, including the Burnett terms and augmented Burnett terms, are computed by using central difference approximations. The additional boundary conditions for the Burnett equations are formulated by using the new method described in this paper. In order to solve the Burnett equations efficiently by using large time steps in the numerical computations, the Burnett stress and heat flux terms and the inviscid flux terms are treated implicitly by using the implicit line Gauss-Seidel iteration method. The details of the numerical method can be found in [25].

Depending on the freestream Knudsen numbers of the flow, CFL numbers in the computations are between  $10^3$  to  $10^8$ , and a computation usually converges after 500 to 1000 iterations.

## V. Flow-Field Burnett Solutions

Hypersonic flow past a cylinder is computed by using the two-dimensional Burnett equations with the new formulation of boundary conditions. For each computational case, we have obtained the Navier-Stokes solutions with the first order slip conditions (N-S), the Burnett equations with the first order slip conditions (Burnett 1) and the Burnett equations with the Schamberg's second order slip conditions (Burnett 2). Since the tangential derivatives of flow variables on the wall are much smaller than the normal derivatives, the Schamberg's second order slip boundary conditions are computed approximately by keeping only the normal derivatives in Eqs. (17) and (18).

Hypersonic flow past a cylinder is chosen as the test case for the Burnett equations because the flow field in the stagnation region is relatively uniform in local Knudsen numbers. Therefore, it is relatively easy to evaluate the Burnett equations together with a set of surface slip boundary conditions with a given free stream Knudsen number. At the same time, the flow near the stagnation region and across the bow shock wave is important for developing future hypersonic vehicles because this area involves the most severe surface heating rates and the most intense radiation. Since the main focus of this paper is on the effect of the translational nonequilibrium on hypersonic flow, the flow is assumed to be monatomic gas without other thermal nonequilibrium.

The flow conditions are chosen to be the same as those for the monatomic gas with a hard-sphere model calculated by Wada, Koura, and Matsumoto<sup>[26]</sup> using the null-collision DSMC method of Koura. The free stream Mach number is  $M_\infty = 10.95$ , the wall of the cylinder is assumed to be a diffuse-reflection cold wall i. e.,  $\sigma = 1$  and  $\alpha = 1$  and  $T_{wall} = T_\infty = 300K$ . The gas is assumed to be a monatomic gas with a hard sphere gas model, i. e.,  $Pr = 2/3$ ,  $\gamma = 5/3$ . The viscosity coefficient of a hard sphere gas model is given by  $\mu = \mu_0(T/T_0)^{0.5}$ , where  $\mu_0 = 2.2695 \times 10^{-5} kg/msec$  and  $T_0 = 300K$ . In this paper, the freestream Knudsen number is defined by  $Kn_\infty = \lambda_\infty/r$ , and  $\lambda_\infty$  is the mean free path and  $r$  is the radius of the cylinder.

Figure 3 shows a schematic of computational domain and a set of  $38 \times 60$  grids. Grid refinement studies have been performed. Two sets of grids with  $76 \times 120$  (case A), and  $152 \times 240$  (case B) grid points have been used to compute the case of  $Kn_\infty = 0.2$ . The computational results show that the stagnation point heating coefficient of case B is about 1.3% higher than that of case A. Therefore, the grid size of case B is considered appropriate and all the results presented in this papers are performed by using the same grid size corresponding to the grids of case A.

### Computational Case 1: $Kn_\infty = 0.2$

Detailed DSMC results by Koura et. al. of the present test case are available for comparison. As pointed by Koura<sup>[27]</sup>, these DSMC results are obtained by using a rectangular grid cells, hence it is difficult for the Monte Carlo method to calculate flow data along the body surface. Consequently, the comparisons for flow parameters along body surface herein are only approximate comparisons.

Figures 4, 5 and 6 show the temperature, velocity and density distributions along the stagnation streamline. The results show that the Burnett equations predict a thicker bow shock wave compared with the Navier-Stokes equations. In all three figures, the Burnett solutions agree better with the DSMC results than the Navier-Stokes equations do. Particularly, the temperature and the velocity distributions show more significant difference between the Burnett and Navier-Stokes results. However, the density distribution dose not show much difference across the shock for the present case of Knudsen number 0.2. For the Burnett equations with first order slip boundary conditions and with Schamberg slip conditions, the results are very close except near the wall surface.

Figures 7, 8 and 9 show the distributions along body surface of heat flux coefficient ( $c_\infty = \sqrt{2RT}$ ), normal pressure coefficient and shear stress coefficient. The differences between the Navier-Stokes solutions and Burnett solutions are not very large for the present case of Knudsen number 0.2. The Burnett heating flux coefficient and shear stress coefficient agree better with

DSMC results. However, all the continuum results under predict the normal pressure coefficient compared with the DSMC results. This discrepancy may be due to the inaccuracy of the DSMC results using a rectangular coarse grid cell on circular surface.

The flow-field temperature contours of the DSMC and Navier-Stokes results are compared in Figure 10, and the temperature contours of the DSMC and Burnett 1 results are compared in Figure 11. Similar comparisons of flow-field density contours are shown in Figures 12 and 13. All the contours show that the Burnett solutions agree much better with the DSMC results than the Navier-Stokes solutions.

The result comparisons show that the Burnett equations with the first-order slip boundary conditions do improve the Navier-Stokes equations results in hypersonic flow past a cylinder when  $Kn_\infty = 0.2$ . On the other hand, the Burnett solutions with the first order slip conditions are not very different from the Burnett solutions with Schamberg slip conditions.

### Flow Parameters vs. Knudsen Numbers

So far, we have computed the flow for five cases of different freestream Knudsen numbers:  $Kn_\infty = 0.02, 0.1, 0.2, 0.3, 0.4$ . The flow conditions and geometry of all these test cases are the same except the free stream pressure and density corresponding to the variation of Knudsen numbers. We examine the effect of translational nonequilibrium on the Navier-Stokes solutions and the Burnett solutions. Since we currently do not have DSMC results for these cases except Case 1, the results of the Burnett solutions are compared with the Navier-Stokes solutions.

Figures 14, 15, and 16 show variations of the surface heat-flux coefficient, normal pressure coefficient, and temperature at the stagnation point with Knudsen numbers  $Kn_\infty$ . Figure 14 shows that as the flow becomes more and more rarefied, the surface heating rate predicted by the Burnett equations with first order slip boundary conditions is lower than those predicted by the Navier-Stokes equations. The Burnett results seem to be in the right direction since the Navier-Stokes equations usually overpredict the stagnation heating rates<sup>[28]</sup>. On the other hand, the Burnett equations with the Schamberg slip boundary conditions start to increase rapidly as Knudsen number gets larger than 0.2. The results show that Schamberg's second slip conditions may not be appropriate because they are not derived by using the Knudsen layer solutions.

Figure 15 shows that the Burnett 1 results predict lower normal pressure than those of the Navier-Stokes equations. Again, Burnett equations with the Schamberg boundary conditions (Burnett 2) do not seem to be correct. Figure 16 shows the temperature on the wall surface at the stagnation point predicted by the Burnett 1 results is very close to the Navier-Stokes results because they use the same first slip boundary con-

ditions. On the other hand, Burnett 2 results predicted much lower surface temperatures. It should be pointed out that the surface temperature and the velocity for the continuum equations are not the same as the actual values on the wall surface.

Since the shear stress is zero at the stagnation point, figure 17 shows the shear stress coefficient on a fixed point on the body surface (45.6 degree from the stagnation point) against the Knudsen number  $Kn_\infty$ . The results show that the shear stresses predicted by the Burnett 1, Burnett 2, and the Navier-Stokes equations are not very different. Figure 18 shows the slip velocity on the surface at the same point. Since Burnett 1 and the Navier-Stokes equations use the same first order slip boundary conditions, the slip velocities of the two solutions are very close. The Burnett 2 results, on the other hand, predict a much lower slip velocity ( $u_s < 0$  when  $Kn_\infty > 0.2$ ) on the wall.

These results show that the Burnett 1 results seem to give improvement over the Navier-Stokes equations, while the Burnett solutions with Schamberg second order slip conditions are not valid for Knudsen number larger than 0.2.

#### Cases 2 and 3: $Kn_\infty = 0.02, 0.4$

Some of the results of case 2 and case 3 are presented as follows.

Figures 19 and 20 are temperature distributions along the stagnation streamline for the Knudsen numbers of 0.02 and 0.4 respectively. For case 2, where the Knudsen number, 0.02, is very small, the Burnett solutions agree well with the Navier-Stokes results as expected. For case 3, the Knudsen number 0.4 is not negligibly small, the Burnett equations predict thicker bow shock than the Navier-Stokes solutions do. On the other hand, the Burnett 2 results give much lower surface temperature than the Burnett 1 results.

Figures 21 and 22 are heat coefficient distributions along the body surface for case 2 and 3 respectively. Again, the Burnett and Navier-Stokes results agree well for case 2. For case 3, the Burnett 1 results predict lower heating rates on the surface than the Navier-Stokes equations, the Burnett 2 results predict slightly higher heating rates on the surface than the Navier-Stokes equations,

Finally, figures 23 and 24 show the temperature contours comparison between the Navier-Stokes and the Burnett 1 results. The Burnett 1 results of case 2 agree very well with Navier-Stokes results except for a small area within the bow shock. On the other hand, the Burnett 1 results of case 3 predict a much thicker shock wave than the Navier-Stokes equations do.

These results show that when the Knudsen number is very small (about 0.02), the Burnett solutions agree very well with the Navier-Stokes equations. These results also indicate that the Navier-Stokes equations are

adequate in that case. On the other hand, as the Knudsen number increases, the Burnett solutions differ from the Navier-Stokes solutions. The Burnett equations with first order slip predict a thicker shock wave and lower stagnation heating rates than the Navier-Stokes equations do.

## VI. Conclusions

A new method in formulating the additional boundary conditions for the Burnett equations has been proposed. The new method requires the same number of physical boundary conditions as the Navier-Stokes equations do, and the additional boundary conditions are obtained by using the Navier-Stokes equations as the leading approximation of the solutions on the boundary. This treatment eliminates the ambiguity of the boundary conditions used in our previous studies. The results show that the flow-field solutions of the Burnett equations can be uniquely obtained by using the present boundary conditions.

The Burnett solutions with the new boundary conditions have been obtained for hypersonic flow past a cylinder. When the Knudsen number is very small (about 0.02), the Burnett solutions agree very well with the Navier-Stokes equations. For test cases with larger Knudsen numbers, the Burnett solutions obtained by using the first-order slip boundary conditions predict lower stagnation heating rates and a thicker bow shock wave than the Navier-Stokes solutions. The comparison of the results shows that the Burnett solutions with first order slip conditions agree better with DSMC results than the the Navier-Stokes solutions in the continuum transition regime.

On the other hand, the Burnett solutions obtained by using the Schamberg boundary conditions do not seem to be correct when the Knudsen number is larger than 0.2. Further studies are needed to derive appropriate second order slip conditions for the Burnett level of approximations. Still, the Burnett equations with the first order slip conditions are able to provide more realistic results when the gas flow starts to be in the continuum transition regime.

## 8. Acknowledgements

This research was supported by AFOSR grant F49620-92-J-0090, with Dr. L. Sakell as the grant monitor. The author would like to thank Dr. K. Koura of National Aerospace Laboratory of Japan for providing detail results of his DSMC calculations.

## References

- [1] H. K. Cheng. Perspectives on hypersonic viscous flow research. *Annu. Rev. Fluid Mechanics*, 25, 1993.

- [2] G. A. Bird. Monte Carlo simulation of gas flows. *Ann. Rev. Fluid Mech.*, 10:11-13, 1978.
- [3] S. Chapman and T. G. Cowling. *The Mathematics Theory of Non-Uniform Gases*. Cambridge University Press, 1960.
- [4] H-S Tsien. Superaerodynamics, mechanics of rarefied gases. *J. of Aero. Sci.*, 13(12), Dec. 1946.
- [5] F. S. Sherman and L. Talbot. Experiment versus kinetic theory for rarefied gases. In F. M. Devienne, editor, *Rarefied Gas Dynamics*, pages 161-191, 1958.
- [6] J. D. Foch. On higher order hydrodynamic theories of shock structure. *Acta physical Austriaca, suppl. X.*, pages 123-140, 1973.
- [7] Samuel A. Schaaf and P. L. Chambre. Flow of rarefied gases. *Princeton Aeronautical Paperbacks*, 8, 1961.
- [8] M. N. Kogan. *Rarefied Gas Dynamics*. New York, Plenum Press, 1969.
- [9] D. R. Chapman, K. Fisco, and F. Lumpkin. Fundamental problem in computing radiating flow fields with thick shock waves. In *SPIE Symp. Innovative Sci. and Technol.*, 1988.
- [10] Kurt A. Fisco. *Study of Continuum Higher Order Closure Models Evaluated by a Statistical Theory of Shock Structure*. PhD thesis, Stanford University, 1988.
- [11] Kurt A. Fisco and Dean R. Chapman. Comparison of Burnett, Super-Burnett, and Monte Carlo solutions for hypersonic shock structure. In *16th International Symposium of Rarefied Gas Dynamics*, 1988.
- [12] F. E. Lumpkin III. *Development and Evaluation of Continuum Models for Translational-Rotational Nonequilibrium*. PhD thesis, Stanford University, March 1990.
- [13] M. N. Kogan. Molecular gas dynamics. *Annual Review of Fluid Mechanics*, 5, 1973.
- [14] X. Zhong, R. W. MacCormack, and D. R. Chapman. Stabilization of the Burnett equations and application to high-altitude hypersonic flows. AIAA paper 91-0770, AIAA, January 1991. Reno, Nevada.
- [15] X. Zhong, R. W. MacCormack, and D. R. Chapman. Evaluation of slip boundary conditions for the Burnett equations with application to hypersonic leading edge flow. September 1991. In the proceeding of 4th International Symp. on CFD, Davis, California.
- [16] F. E. Lumpkin III and D. R. Chapman. Accuracy of the Burnett equations for hypersonic real gas flows. AIAA Paper 91-0771, AIAA, 1991.
- [17] G. C. Pham-Van-Diep, D. A. Erwin, and E. P. Muntz. Testing continuum descriptions of low-mach-number shock structures. *Journal of Fluid Mechanics*, 232:403-413, 1991.
- [18] R. Schamberg. *The Fundamental Differential Equations and the Boundary Conditions for High Speed Slip Flow*. PhD thesis, California Institute of Technology, Pasadena, California, 1947.
- [19] N. K. Makashev. On the boundary conditions for the equations of gas dynamics corresponding to the higher approximations in the Chapman-Enskog method of solution of the Boltzmann equation. *Fluid Dynamics (Translated From Russian)*, 14(3), May-June 1979.
- [20] C. S. Wang Chang and G. E. Uhlenbeck. On the transport phenomena in rarefied gases. *Studies in Statistical Mechanics*, V:1-17, 1948.
- [21] E. H. Kennard. *Kinetic Theory of Gases*. McGraw-Hill Book Co., Inc., New York, 1938.
- [22] D. J. Alofs and G. S. Springer. Cylindrical Couette flow experiments in the transition regime. *The Physics of Fluids*, 14(2), February 1971.
- [23] M. Van Dyke. *Perturbation Methods in Fluid Mechanics*. The Parabolic Press, Stanford, California, 1975.
- [24] R. W. MacCormack. Current status of numerical solution of the Navier-Stokes equations. AIAA Paper 85-0032, AIAA, January 1985.
- [25] X. Zhong. *Development and Computation of Continuum Higher Order Constitutive Relations for High-Altitude Hypersonic Flow*. PhD thesis, Stanford University, July 1991.
- [26] Y. Wada, K. Koura, and H. Matsumoto. Comparison of hypersonic rarefied flows around a circular cylinder between Navier-Stokes and direct-simulation Monte Carlo solutions. In *Book of Abstract, 18th International Symposium on Rarefied Gas Dynamics, Vancouver, Canada*, July 1992.
- [27] K. Koura. Private communication. April 1993.
- [28] J. N. Moss. Non-equilibrium thermal radiation for an aeroassist flight experiment. AAS Preprint AAS-86-348, American Astronautical Society Publication, 1986.

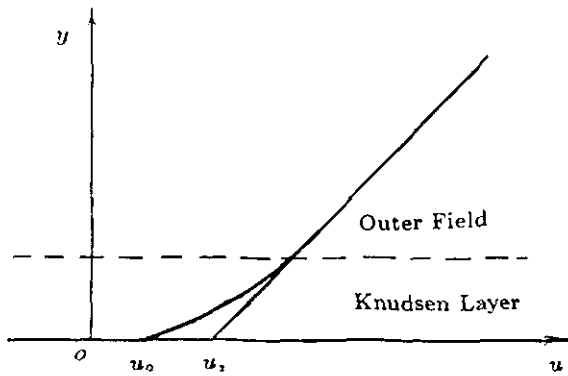


Figure 1: A schematic of velocity distribution across the Knudsen layer and outer field near the wall.

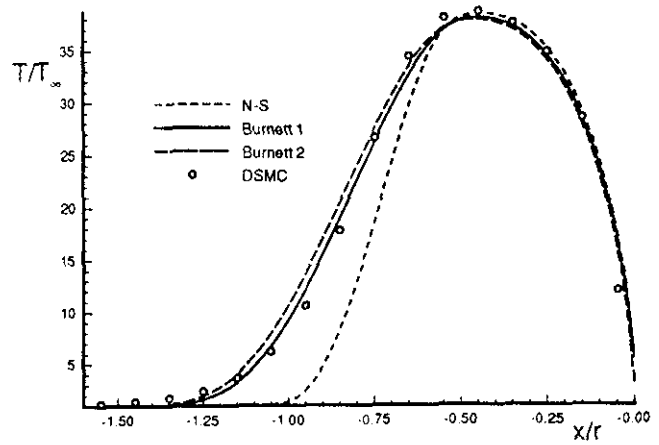


Figure 4: Temperature distribution along the stagnation streamline (Case 1:  $M_\infty = 10.95$ ,  $Kn_\infty = 0.2$ ).

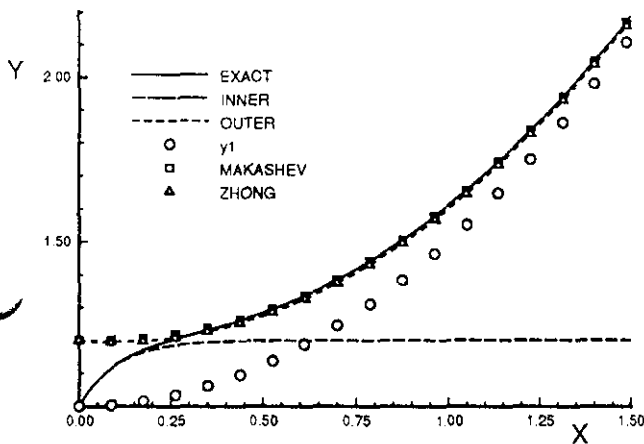


Figure 2: Solutions of the ordinary differential equation in Section III ( $\epsilon = 0.1$ ).

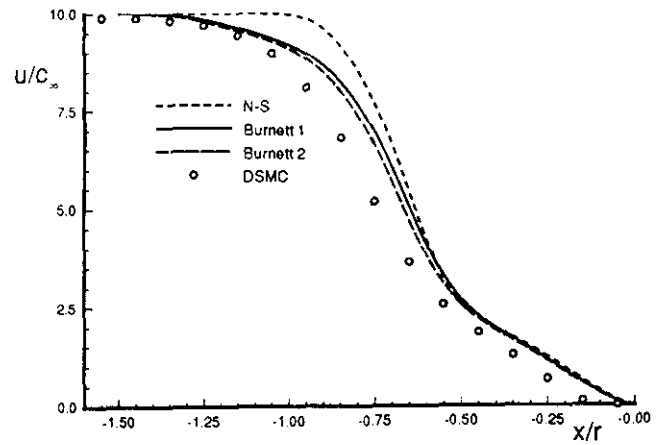


Figure 5: Velocity distribution along the stagnation streamline (Case 1:  $M_\infty = 10.95$ ,  $Kn_\infty = 0.2$ ).

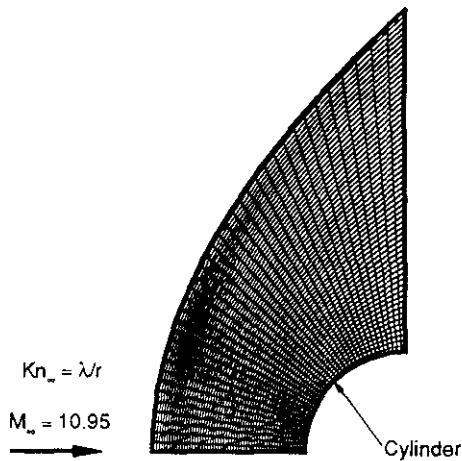


Figure 3: A schematic of the computational domain with a set of  $38 \times 60$  grids.

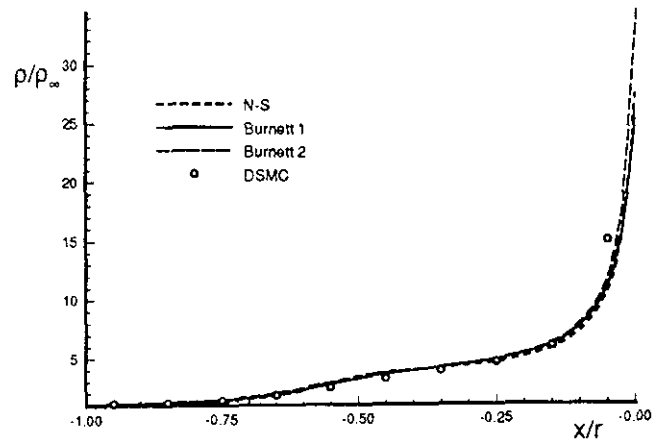


Figure 6: Density distribution along the stagnation streamline (Case 1:  $M_\infty = 10.95$ ,  $Kn_\infty = 0.2$ ).

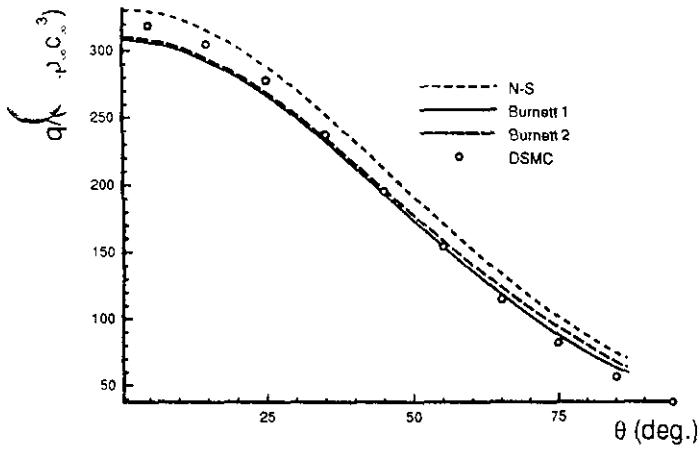


Figure 7: Heat-flux coefficient distribution along body surface (Case 1:  $M_\infty = 10.95$ ,  $Kn_\infty = 0.2$ ).

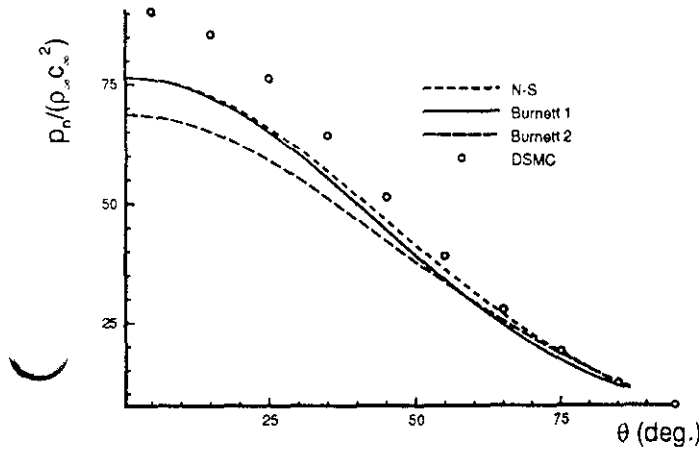


Figure 8: Normal pressure coefficient ( $p_n = p + \sigma_n$ ) distribution along body surface (Case 1:  $M_\infty = 10.95$ ,  $Kn_\infty = 0.2$ ).

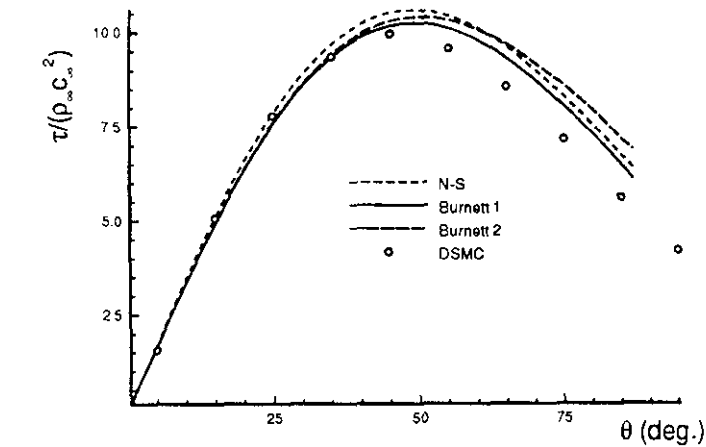


Figure 9: Shear stress coefficient distribution along body surface (Case 1:  $M_\infty = 10.95$ ,  $Kn_\infty = 0.2$ ).

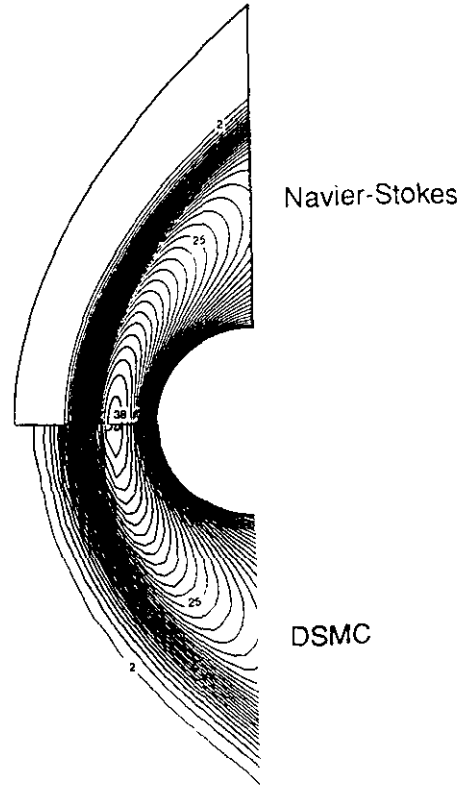


Figure 10: Flow-field temperature ( $T/T_\infty$ ) contours comparison (Case 1:  $M_\infty = 10.95$ ,  $Kn_\infty = 0.2$ ).

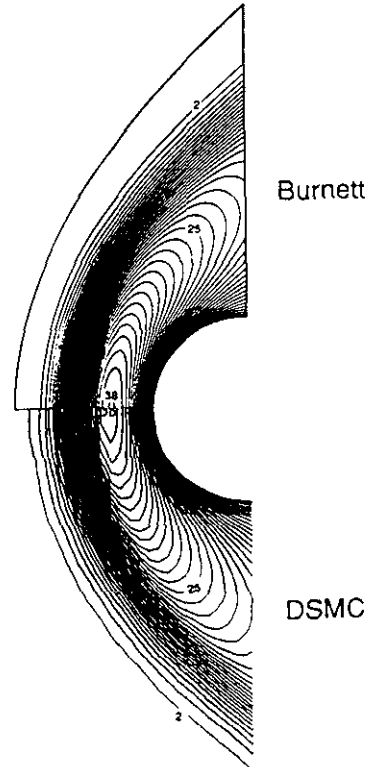


Figure 11: Flow-field temperature ( $T/T_\infty$ ) contours comparison (Case 1:  $M_\infty = 10.95$ ,  $Kn_\infty = 0.2$ ).

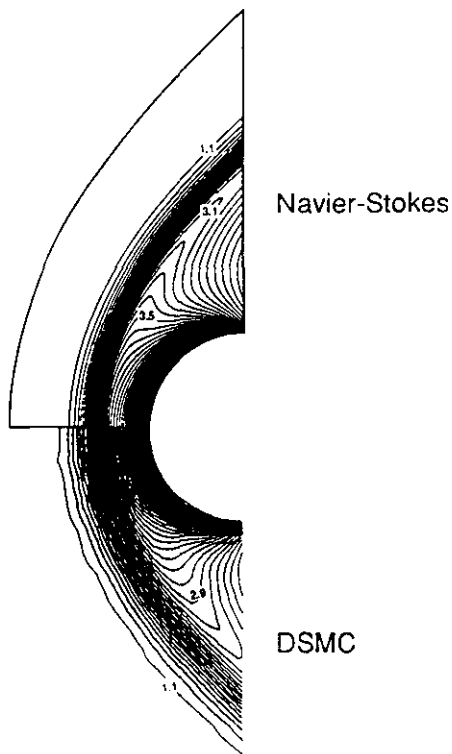


Figure 12: Flow-field density ( $\rho/\rho_\infty$ ) contours comparison (Case 1:  $M_\infty = 10.95$ ,  $Kn_\infty = 0.2$ ).

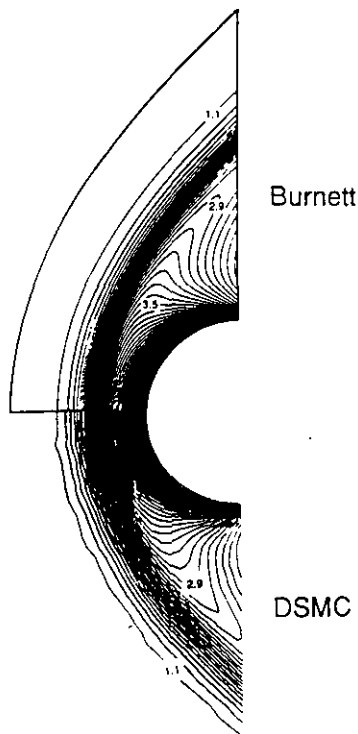


Figure 13: Flow-field density ( $\rho/\rho_\infty$ ) contours comparison (Case 1:  $M_\infty = 10.95$ ,  $Kn_\infty = 0.2$ ).

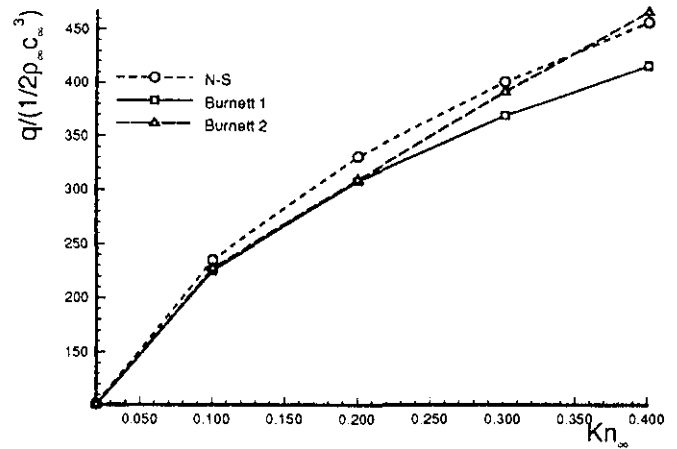


Figure 14: Variation of surface heat-flux coefficient at the stagnation point with Knudsen number for cylinder.

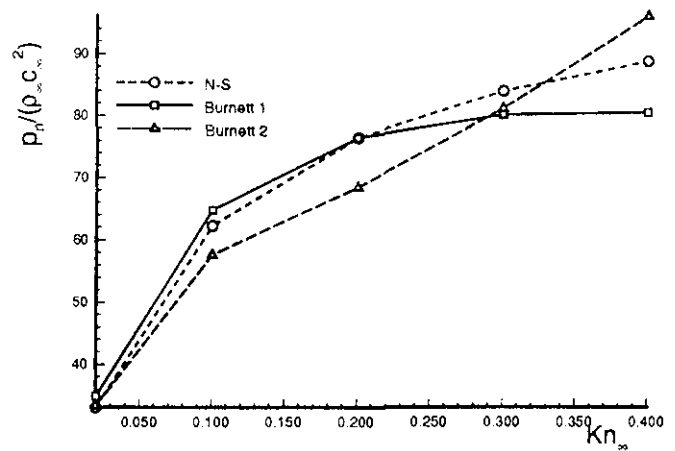


Figure 15: Variation of normal pressure coefficient at the stagnation point with Knudsen number for cylinder.

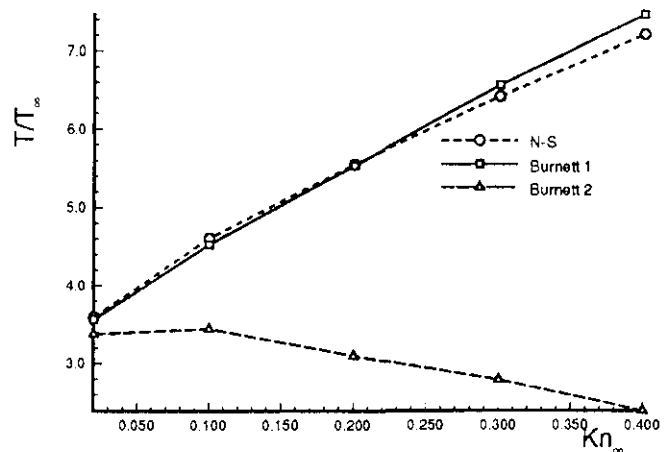


Figure 16: Variation of surface gas temperature at the stagnation point with Knudsen number for cylinder.

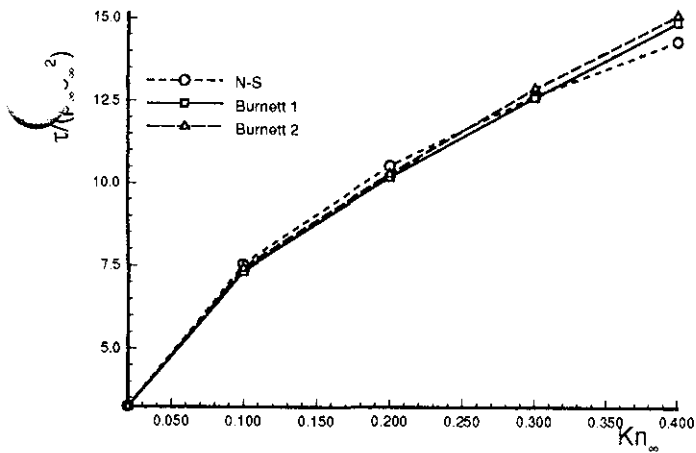


Figure 17: Variation of shear stress coefficient at a fixed point on the body surface ( $45.6^\circ$  from the stagnation point) with Knudsen numbers.

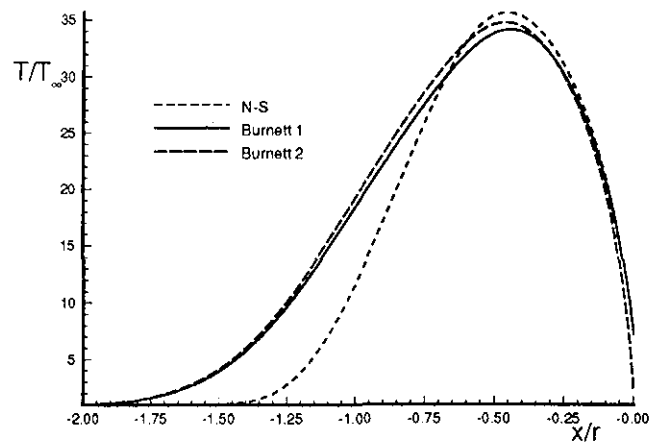


Figure 20: Temperature distribution along stagnation streamline (Case 3:  $M_\infty = 10.95$ ,  $Kn_\infty = 0.4$ ).

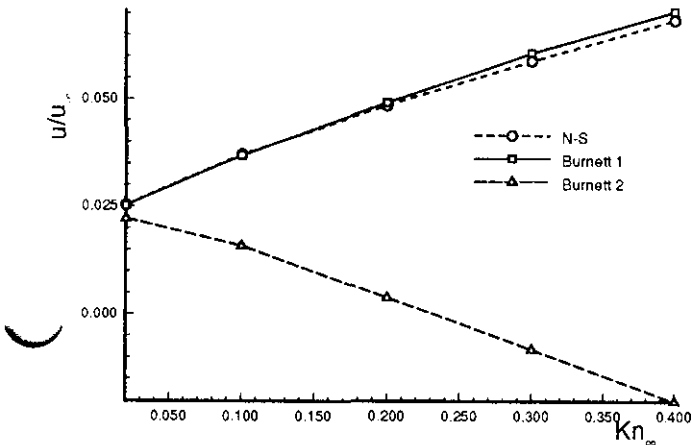


Figure 18: Variation of slip velocity at a fixed point on the body surface ( $45.6^\circ$  from the stagnation point) with Knudsen number.

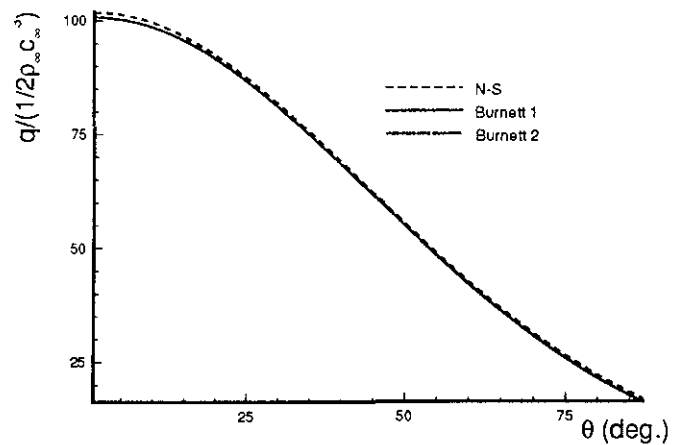


Figure 21: Heat-flux coefficient distribution along body surface (Case 2:  $M_\infty = 10.95$ ,  $Kn_\infty = 0.02$ ).

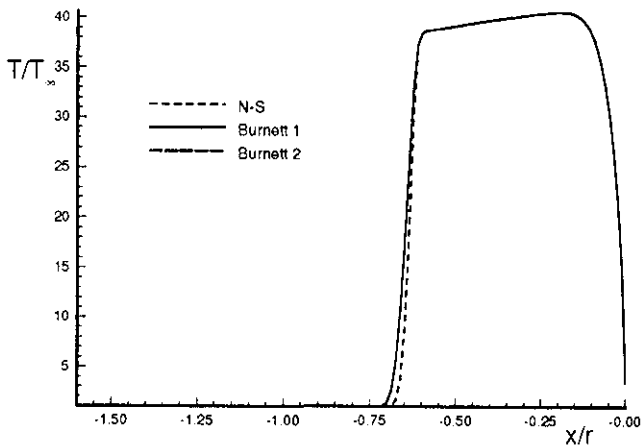


Figure 19: Temperature distribution along stagnation streamline (Case 2:  $M_\infty = 10.95$ ,  $Kn_\infty = 0.02$ ).

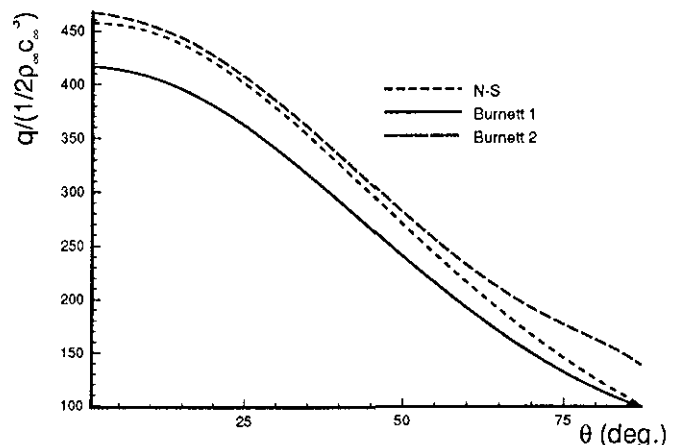


Figure 22: Heat-flux coefficient distribution along body surface (Case 3:  $M_\infty = 10.95$ ,  $Kn_\infty = 0.4$ ).

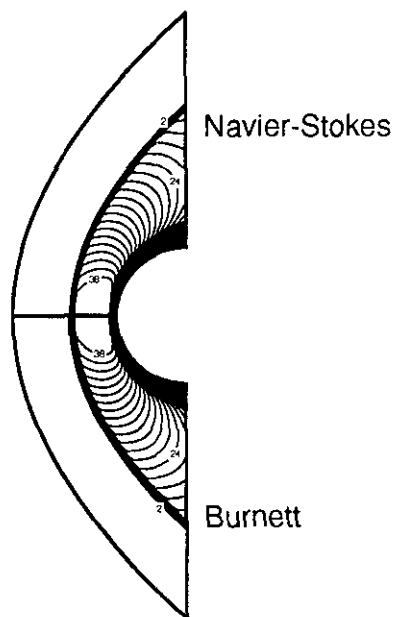


Figure 23: Temperature ( $T/T_\infty$ ) contours comparison for the case of  $M_\infty = 10.95$ , and  $Kn_\infty = 0.02$ .

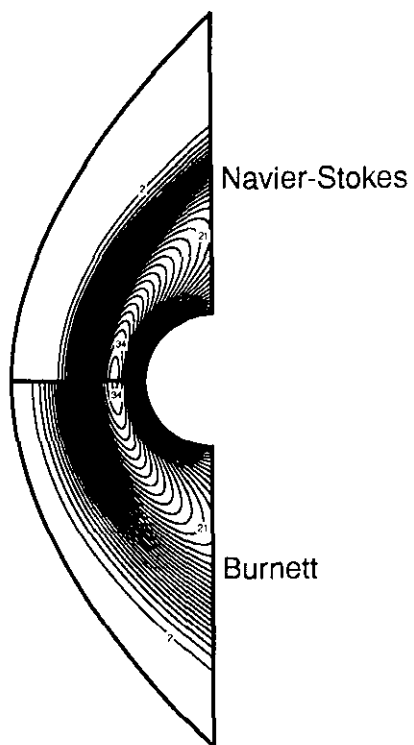


Figure 24: Temperature ( $T/T_\infty$ ) contours comparison for the case of  $M_\infty = 10.95$ , and  $Kn_\infty = 0.4$ .